Title: Non-invasive High-Intensity Focused ultrasound treatment of Twin-Twin Transfusion Syndrome: a preliminary *in vivo* study

Authors: Caroline J. Shaw[1,2], John Civale[3], Kimberley J. Botting[1], Youguo Niu[1], Gail ter Haar[3], Ian Rivens[3], Dino A. Giussani[1], Christoph C. Lees[2,4*]

Affiliations:

[1] Department of Physiology, Development and Neuroscience, University of Cambridge, CB2 3EG, UK

[2] Institute of Reproductive and Developmental Biology, Imperial College London, W12 0HS, UK

[3] Joint Department of Physics, Institute of Cancer Research, Sutton, SM2 5NG, UK

[4] Department of Obstetrics and Gynaecology, University Hospitals Leuven, 3000 Leuven, Belgium

*Corresponding author: Christoph.lees@imperial.nhs.uk

One Sentence Summary: High intensity focused ultrasound can ablate blood flow in the sheep placenta and is potentially translatable to human twin twin-transfusion syndrome, where the invasive nature of current treatments limit their value.

Abstract:

We investigated the efficacy, materno-fetal responses, and safety of using high-intensity focused ultrasound (HIFU) for non-invasive occlusion of placental vasculature compared to sham treatment in anesthetised pregnant sheep. This technique for non-invasive occlusion of placental vasculature may be translatable to the treatment of conditions arising from abnormal placental vasculature, such as Twin-Twin Transfusion Syndrome (TTTS). Eleven pregnant sheep were instrumented with maternal and fetal arterial catheters and time transit flow probes to monitor cardiovascular, acid-base, and metabolic status, then exposed to HIFU (n=5) or sham (n=6) ablation of placental vasculature through the exposed uterine surface. Placental vascular flow was occluded in 28/30 targets, and histological examination confirmed occlusion in 24/30. In both HIFU and sham exposures, uterine contact reduced maternal uterine artery flow, but delivery of oxygen and glucose to the fetal brain remained normal. HIFU can consistently occlude in vivo placental vessels and ablate blood flow in a pregnant sheep model. Cardiovascular and metabolic fetal responses suggest that the technique is safe in the short term and potentially translatable to human pregnancy.

Introduction

High-intensity focused ultrasound (HIFU) (1) is a clinically approved therapeutic technique for non-invasive ablation of uterine fibroids, as well as bony and soft tissue cancers. Ultrasound waves generated by a shaped piezoelectric ceramic transducer, positioned outside the body, produce localized tissue destruction at depth, using a combination of thermal and/or pressure effects (2). Converging ultrasound waves pass through overlying tissue, causing damage where energy is focused, to create a small lesion (typically ellipsoidal, 1-2 mm in diameter and 8-15 mm in length). Combined with diagnostic imaging to target the focus, lesions can be placed adjacent to each other to destroy larger volumes of tissue. Only one successful use of HIFU in human fetal medicine has been reported so far: HIFU soft tissue ablation of the cord insertion in a compromised fetus with twin reversed arterial perfusion (TRAP) sequence, which afforded a better prognosis for the surviving twin (3).

Twin-twin transfusion syndrome (TTTS) affects 10-15% (4) of monochorionic diamniotic (MCDA) twins, has an untreated mortality >80% (5), and is the leading cause of death and disability in twins (6). It results from abnormal vascular connections (predominantly arterio-venous anastomoses, or AVAs) in monochorionic placentae, which allow unequal sharing of placental blood flow (7). Treatment to divide the twins' circulations is recommended in severe (stage 3-4) TTTS (8), where fetal compromise has already occurred (9).

Fetoscopic laser occlusion of placental anastomoses to divide the fetal circulations has been developed over the last 20 years (10). Although neurological outcomes at 2 years may be improved with this technique, meta-analysis has not shown an improvement in survival (11). Complications are secondary to the invasive nature of the procedure, because fetoscopy alone is recognized to worsen neonatal outcomes (9, 12-14); this limits the use of fetoscopic laser to cases of TTTS where

fetal compromise has already occurred. AVAs typically lie deep within the placenta (15), but laser ablation is limited to a maximum depth of a few millimeters; residual anastomoses are visualized using color Doppler in 15-30% cases (16). This may result in recurrent disease (17) or a related condition, twin anemia-polycythemia sequence (TAPS), which is three times more common after laser treatment (13). A non-invasive method which could divide placental circulations and occlude superficial or deep anastomoses could potentially reduce the risks of both procedure-related complications and incomplete vascular occlusion, offering a more effective therapy and widening the scope of treatment. The use of HIFU to specifically occlude placental vasculature is a previously unreported application of the technology.

The aim of this study was to test the efficacy, feasibility, and fetal-maternal safety of ultrasound-guided HIFU placental vascular occlusion in a pregnant animal model as a precursor to human clinical trials. This study required a model of placental vascular anastomoses: AVAs are 0.3-0.6 mm in diameter, and veno-venous anastomoses may be up to 3.5 mm in diameter (18). The pregnant sheep cannot provide a true model of TTTS, because vascular anastomoses between allantoic circulations in multiple pregnancies in sheep are rare (19), unlike in human monochorionic placentation, where they occur in 90% of cases (20). Unlike the discoid human placenta, the sheep placenta is organized into discrete regions of maternal and fetal tissue called placentomes, regions of enmeshed maternal and fetal villi, where materno-fetal countercurrent flow and hemotrophic exchange takes place (21). Fetal vessels arise from the placentomes and are up to 5 mm in diameter. These run between placentomes before joining together to form the umbilical cord, providing appropriately sized target vessels.

In the human placenta, fetal cotyledons are recognized, with discrete villous trees of fetal blood flow where concurrent flow and hemotrophic materno-fetal exchange occurs, despite the

externally continuous nature of the placental surface. The villous trees of both human and sheep placentae are similar in that they contain stem, intermediate, and terminal villi of comparable structure and size (22). Hence, although the human and sheep placentae initially appear very different, they are functionally comparable and their vasculature is anatomically similar, and the pregnant sheep model has been used previously to demonstrate intrauterine fetoscopic laser ablation of placental vasculature (23).

Unlike other experimental animal models, sheep tend to have singleton or twin pregnancies, and the birth weight of a lamb is similar to that of a human baby. Furthermore, sheep and humans have comparable anatomy of the heart and vasculature, and the temporal development of the cardiovascular system is similar (24). The gestational time for the ewe is 145-150 days, around 50% of the human gestational period, but longer than many other experimental animals, meaning that techniques, timing, and duration of experimentation are more easily translated from research to a clinical context.

Results

Efficacy and safety of HIFU placental vascular occlusion

Based on comparison of pre- and post-exposure color Doppler imaging, HIFU successfully ablated blood flow in 28 of 30 (93.3%) placental vessels (Fig. 1A,B). Of the 28 successful ablations, 27 were achieved in a single exposure series; 2 of the 3 remaining placentomes were re-exposed, resulting in 1 further successful ablation (total 32 exposure series). During exposures, hyperechoic regions (Fig. 1C) were seen to develop at the HIFU focus with harmonic imaging. The appearance of two or more successive hyperechoes in an exposure series was associated with successful ablation of blood flow in 28 of 28 successful HIFU exposure series and 0 of 4 unsuccessful ones. This was a more sensitive indicator for monitoring treatment with harmonic imaging than placentome structural change, which was only seen in 15 of 28 successful ablations.

Treatment success was assessed using 3 measures. The primary measure was new onset absence of flow on color Doppler after exposure ("no flow"), because this is the measure available clinically to judge success and guide therapy. The study design allowed secondary confirmation to be sought from macroscopic observation and histological examination of damaged tissue in the targeted region. As already mentioned, treatment success defined by "no flow" was 93.3%.

Gross pathological changes after HIFU exposure were observed macroscopically in the central region of all 30 targeted placentomes, with either tissue darkening (Fig. 2A) or tissue pallor (Fig. 2B), in some cases extending into the peripheries. This included the 2 in which flow was not successfully occluded. Histological examination of damaged tissue was possible in 26 of 30 placentomes; in 2 placentomes (<2 cm diameter) there was extensively damaged tissue, rendering them too friable to be sectioned for H&E staining. In the remaining 2 placentomes, no clear view of the origin of fetal vessels could be seen in the sections. Evidence of clot within fetal vessels,

suggestive of occlusion, was found in 24/26 (92.3%) specimens and was not found in 2/26 (8.7%) or in sham treated placentomes (Fig. 2C,D). The 2 placentomes without evidence of vessel occlusion were the same 2 in which color flow Doppler signals were still present on the post-treatment images. Outcomes are summarized in table S1.

A single case of vessel hemorrhage in the 30 placentomes targeted (3.3%) was associated with equipment malfunction. The automated gantry failed to move and delivered 4 exposures to the same position in the vessel wall. We were not able to resolve the hemorrhage non-invasively, but all fetuses survived the experimental protocol despite this one incident. No damage to the uterus, adjacent maternal structure, or fetus was observed in this study, based on external examination at post mortem.

Maternal cardiovascular, acid-base, and metabolic responses to HIFU exposures

In both HIFU and sham ablation studies, there was a reduction in uterine artery blood flow by up to 30% of basal flow, secondary to increased uterine artery vascular resistance during the period of time when the HIFU and sham exposures were being applied; the maternal mean arterial blood pressure and heart rate remained unchanged throughout the procedure (Fig. 3). Given that this reduction in blood flow had a similar time of onset and magnitude in both HIFU and sham ablations, the only common potentially causative event which occurred in both groups at this point in the experiment was the gentle handling and manipulation of the uterus to optimize the acoustic window. B-Mode/Doppler ultrasound was used during both the baseline and treatment phases of the experimental protocol and thus is unlikely to be the causative factor. Values for metabolic and acid-base status were not different between treatment groups at baseline and remained

predominantly unchanged during the experimental procedures involving both sham and HIFU exposures (Table 1).

Fetal cardiovascular, acid-base, and metabolic responses to HIFU exposures

The fetal heart rate and mean arterial blood pressure remained constant throughout the experimental procedure (Fig. 4). Blood flow to the fetal brain was unchanged in terms of absolute volume, and oxygen and glucose delivery to the fetal brain both remained within expected parameters and were unaltered during the experimental procedure, despite a reduced partial pressure of oxygen (P_aO_2) in the fetal blood by the end of the recovery period. (Fig. 4, Tables 2 and 3). By the end of the recovery period, there was a gradual deterioration of fetal acid-base and metabolic status, which was not different in HIFU compared to sham groups, and these changes occurred at the same time points for both (Table 2).

There was a reduction in fetal femoral artery blood flow volume and an increase in femoral artery vascular resistance, which occurred in conjunction with the reduction in maternal uterine artery blood flow (Fig. 3 and 4). There was also an increase in the ratio of blood flow between the fetal carotid and femoral arteries (Fig. 4).

The median duration of anesthesia at the start of the experimental protocol (start of baseline recording) was 145 min (range 128-180 min) in the sham group and 138 min (range 125-157 min) in the HIFU group. This was not significantly different ($p=0.14$), and values for maternal and fetal cardiovascular, metabolic, and acid-base status during baseline recordings (Table 1 and 2) were not different between exposed and sham groups, demonstrating that this difference in anesthesia time was not clinically important.

Discussion

This study demonstrates the potential for the use of HIFU as a non-invasive method of placental vascular occlusion in pregnant sheep, an animal model that mimics vascular anastomoses in the monochorionic human placenta. The primary aims of this study were to assess the efficacy and safety of this technique for the mother and fetus. To this end, the recorded maternal and fetal cardiovascular, acid-base, and metabolic responses secondary to ultrasound-guided HIFU placental vascular occlusion were encouraging.

The main impact on maternal physiology was a modest fall in uterine artery blood flow during the treatment phase of the experimental protocol in both HIFU and sham exposure series. The only experimental feature related temporally to this fall in uterine blood flow was the uterine handling needed to alter uterine position to optimize the acoustic window during the treatment phase. This was necessary to optimize the path for the ultrasound beam to follow, given the artificial introduction of intra-abdominal air by the preceding laparotomy, to produce vascular occlusion in the targeted placentomes. The effect of direct intraoperative uterine contact and handling on fetal wellbeing and physiology has not previously been reported. An acute, anesthetic-related reduction in uterine artery blood flow secondary to maternal bradycardia and arterial hypotension has been linked to isoflurane usage (25-31), however, this response is time-dependent, and all parameters recovered to baseline within 120 minutes of start of anesthesia in these studies (25, 26). The maternal and fetal cardiovascular parameters in our study were within normal ranges at the start of the experimental protocol (start of baseline), as would be expected based on this previously published work, and isoflurane delivery remained stable throughout the experimental protocol. It is thus unlikely to account for the fall in uterine artery blood flow observed here. Maternal heart rate and arterial blood pressure remained stable through the experimental

procedure, so the primary cause of reduced blood flow in the uterine artery in this setting may be increased resistance in the uterine artery secondary to local vasospasm, rather than autoregulation associated with system-wide maternal cardiovascular alterations which have been reported under anesthesia (32).

Fetal peripheral vasoconstriction, although classically understood as part of the fetal brain sparing response to acute hypoxia (33), can also result from fetal acidosis in the absence of fetal hypoxia (34), primarily mediated by the sympathetic nervous response and maintained by endocrine-mediated fetal stress responses (35). Peripheral vasoconstriction has been described in sheep fetuses as a response to reduced uterine blood flow in the absence of fetal hypoxia (36). Isoflurane sedation does not alter the capacity of fetal sheep to redistribute cerebral and systemic blood flow in response to reduced utero-placental flow or the development of acidosis (29). Accordingly, fetal peripheral vasoconstriction responses of the same magnitude were observed in both groups in response to the reduction in uterine artery blood flow. These fetal changes persisted beyond the normalization of uterine artery blood flow in the recovery period. It is important to note that these responses were not worsened by the addition of HIFU placental vascular occlusion, and there was no corresponding increase in carotid blood flow during this period to suggest cerebral vasodilation (33, 37). The cerebral vasodilation aspect of the fetal brain sparing response to acute hypoxia is under paracrine, rather than systemic, control (33). Given that the delivery of oxygen and glucose to the fetal brain was preserved within normal limits for the duration of all experiments, hypoxia-induced cerebral vasodilatation would not be expected. Therefore, the increase in the ratio of the carotid to femoral blood flow in the fetus is secondary to the fall in femoral blood flow, most likely as a result of increased sympathetic outflow in response to the

uterine vasospasm, rather than being representative of cerebral vasodilation and peripheral vasoconstriction in response to acute fetal hypoxia (37).

Although fetal oxygenation remained within normal limits for the duration of the procedure, there was a gradual reduction in the fetal P_aO_2, the saturation of oxyhemoglobin, and delivery of oxygen to the brain between the baseline and recovery periods. These changes were not different between HIFU and sham groups and are more likely to represent fetal deterioration under anesthetic than an effect of HIFU exposures. Mechanical ventilation was used to maintain the ewes in an isocapnic state despite the need for periods of breath holding; however, a mixed respiratory and metabolic fetal acidosis still developed. Placental transfer of oxygen relies on the double Bohr effect, where elimination of carbon dioxide (CO_2) from the fetal circulation drives maternal oxyhemoglobin disassociation and increases the affinity of fetal hemoglobin for the oxygen. Anything that reduces fetal elimination of CO_2, resulting in a fetal respiratory acidosis, paradoxically reduces the availability of maternal oxygen at the placental interface. A progressive fetal respiratory acidosis and falling P_aO_2 has been reported in the anesthetized fetus regardless of concomitant operative or experimental procedures (25, 26), and the P_aCO_2 at the end of our recovery period is comparable to other published values for this duration of isoflurane anesthesia. We suggest that these changes in fetal pH as a result of anesthesia are what underlie the trend to reduced oxygenation seen in our results.

Carbon dioxide is generated by the fetus at a steady rate and is eliminated from the fetal circulation by diffusion across the placenta.(38) Elevated maternal P_aCO_2 causes steady state equilibration (Fick's first principle) to reset to a higher baseline, eliminating less CO_2 from the fetus. (38) Although there was no increase in maternal P_aCO_2 observed during the experimental protocol, the maternal baseline was above the normal range for non-anesthetized sheep.

Ventilating sheep in the recumbent position and their increased alveolar dead space compared to humans make CO_2 elimination from the ovine lungs less effective under anesthesia (39-41), resulting in a mild maternal respiratory acidosis.

The placental exchange rate of CO_2 is also affected by the supra-physiological P_aO_2 in the mother and fetus. The Haldane effect describes the increased capacity of deoxygenated hemoglobin to buffer CO_2 compared to oxygenated hemoglobin (42), and this has been calculated to account for 46% of placental CO_2 exchange.(38) The artificially elevated concentrations of oxygenated hemoglobin in both mother and fetus reduce the magnitude of the Haldane effect in this setting, and so further reduce the fetal elimination of CO_2. CO_2 diffusion across the placenta is limited by uterine blood flow (39) because it is highly soluble (42), so the additive effect of reduced uterine artery blood flow during the period of uterine manipulation accelerates the increase in fetal CO_2 accumulation. Decreases in fetal pH in our results were augmented by the fetal peripheral vasoconstriction observed: lactate is a product of anaerobic respiration and is produced in greater quantities by the under-perfused fetal tissues during peripheral vasoconstriction, particularly by the muscle bulk of the hind limbs, and it increased by the recovery period of the experiment, contributing to a mixed respiratory and metabolic acidosis (43).

Collectively, these findings suggest an appropriate fetal defense response, allowing compensation for a non-hypoxic challenge, rather than fetal distress resulting from HIFU. Given that HIFU has already been used in human pregnancy for the treatment of TRAP sequence (3), these findings already have relevance to clinical obstetrics. It should be noted that the sheep fetuses were healthy and that the effects on a fetus compromised by TTTS may be different. However, one aim of developing a non-invasive method to divide fetal circulations is to reduce the risks

associated with the invasive nature of current therapies and to allow earlier intervention before such fetal compromise occurs.

This study has demonstrated that placental vessels can be identified and targeted for HIFU ablation using color Doppler ultrasound in the sheep. Non-invasive color flow Doppler ultrasound improves the accuracy of HIFU targeting when compared to surgical exposure or visual identification of blood vessels (44). Targeting accuracy worse than 3 mm (45) can result in failed vascular occlusion and injury to adjacent structures such as bowel (46, 47), nerves (48), or other blood vessels (49). Our treatment protocol, which places a linear track of 4-7 exposures across each vessel, involves a 6-12 mm linear movement of the automated gantry across the intended target and should be tolerant of a small degree of inaccuracy in targeting placental vessels. Placental vessels can be readily identified using Doppler ultrasound in sheep, and Doppler velocimetry correlates well with absolute flows measured invasively in these vessels (50, 51). AVAs in human monochorionic placentae have been successfully identified using color and pulsed wave Doppler, with a sensitivity of 25-50% when compared to placental injection studies (52-54). In all cases, identification was easier with an anterior placenta, which may be a more accessible target for HIFU exposures than a posterior placenta when a fixed focal length HIFU transducer is used.

The treatment protocol used shows that HIFU can consistently (93.3%) ablate in vivo placental blood flow in a pregnant sheep model, in vessels with clinically relevant diameters. Although the protocol used did not achieve occlusion in every target, it is a strength of our technique that treatment success and failure can be assessed in real time by the same modality (color Doppler) used to target HIFU, and residual anastomoses may be suitable for immediate retreatment. Residual anastomoses are identified by color Doppler imaging in 15-30% of cases

after laser therapy (16) and may lead to recurrent disease with a worse overall prognosis (17) or a threefold increased incidence of a related condition, TAPS (13). Residual anastomoses may not be identified during laser treatment and would require a further invasive treatment to resolve, which is currently not recommended. Recently, fetoscopic laser has changed from selective coagulation of vessels where they cross the "vascular equator" to bipartition of the placenta. In this procedure, additional laser ablation of placental tissue is used to join the sites where vessels have been coagulated and to create a physical separation between the twins' circulations. This does improve neonatal survival and decreases rates of recurrence and TAPS, however it is associated with an 11.5% double twin loss rate, typically related to the invasive nature of fetoscopic laser (55). Although the anatomy of the sheep placenta lends itself to selective coagulation of vessels because the tissue is discontinuous, the HIFU positioning system is capable of placement of exposures to form a confluent line of tissue destruction along a predetermined track, such as would be required for bipartition of the placenta, making either approach feasible.

Vascular occlusion typically requires higher levels of HIFU energy than ablation of soft tissue (56), and carries with it the potential complications of vessel rupture and hemorrhage, attributed to rapid changes in tissue pressure (46, 48, 57) or accumulation of excessive thermal energy in the vessel wall (58-60). This presents the possibility that the energy levels required to occlude vessels may also cause vessel wall rupture. In our optimization studies, ultrasound exposure intensities higher than used in this study did produce vessel hemorrhage (61) and maximum thresholds were determined, resulting in the optimized protocol presented here. Because of these safeguards, the single incident of vessel wall rupture observed in this study was associated with unintentional non-movement of the gantry, resulting in over-exposure of a single region of the vessel wall. This happened only after 4 repeated exposures in the same location,

suggesting a large safety margin in the upper dose threshold. By limiting the size of the target volume, and thus the total dose delivered to the tissue, our protocol is able to successfully and consistently occlude placental vasculature in this setting, without crossing the threshold at which vascular rupture and hemorrhage occurs. Larger vessels are typically protected from rupture by their thicker walls and higher flow with greater cooling effect (62); one of the treatment failures was an attempt to occlude a larger vessel, and although this was unsuccessful, it was not associated with vascular hemorrhage. Concerns have also been expressed about repeat exposure of vessels resulting in vascular rupture (58-60). In this study, only 2 treatments were repeated, limiting our ability to discuss the value and safety of retreatment. The first of these was successful, although tissue damage spread into the periphery, reaching the capsule of the placentome. This might be considered to have breached a theoretical "safety margin" designed to protect adjacent structures. Despite this limitation, there was no maternal, uterine, or fetal damage or damage to adjacent placentomes. The second retreatment attempted to ablate flow in a case of vessel hemorrhage, and was not successful in either ablating flow or in resolving the vessel hemorrhage. This suggests that an additional protocol of HIFU treatment different from the one currently used should be applied for the case of inadvertent vascular hemorrhage, and this will require future studies before attempting human application.

The energy levels required to occlude placental vasculature (table S2) also present the possibility of pre-focal (maternal skin, abdominal fat, uterus) and post-focal (fetus) damage to structures in the path of the ultrasound energy. The potential for such damage is a consequence of the focused beam geometry, and shorter focal lengths and higher intensities may increase the risk. Although there were no such complications in this study, the range of intensities used was at the higher end of those reported to produce vascular occlusion (56), so there is potential to reduce

these energy levels in future applications. There is also the possibility of lateral thermal spread outside the intended focal zone, as with any energy source that heats tissue, although HIFU exposures of soft tissue typically produce sharply demarcated lesions (63). Again, there were no such complications in this study. There are without doubt important technical considerations with regard to appropriate case selection and careful treatment planning of HIFU exposures to minimize these risks. However, these should be balanced against the potential benefits to mother and fetus of avoiding fetoscopy. Other potential difficulties still remain to be addressed before a human treatment could be implemented. The protocol, transducer, and control software used in these preliminary experiments are not yet optimized for use in human pregnancy, and the need for an adequate acoustic window after surgical instrumentation meant that HIFU was applied directly through the uterine surface rather than through the maternal skin. Delivering HIFU energy truly non-invasively (through intact skin) to achieve vascular occlusion is an essential challenge still to be met and will need to be the subject of future experimental studies. As previously discussed, placental vascular anastomoses can be detected non-invasively by color Doppler, and as demonstrated in our results, color Doppler is an appropriate targeting and treatment monitoring modality for HIFU exposures. The work of Okai et al (3) demonstrates that adequate HIFU energy can be delivered using a transdermal approach into the intrauterine space to ablate soft tissue at the cord insertion in human pregnancy, demonstrating the feasibility of our intended work.

Another key feature of translating these techniques to human pregnancy will involve greater understanding of the mechanisms by which vascular occlusion is produced in this protocol, to allow customization of any potential treatment system for human pregnancy. HIFU can interact with blood vessels to produce vascular occlusion by thermal mechanisms (56). Tissue heating can cause shrinkage of vessel walls (64), narrowing of vessel lumen (65), and/or fusion of the walls in

a closed position (66). HIFU can also damage the vascular endothelium, producing occlusive thrombus that causes permanent obliteration of the vessel through chronic inflammatory processes (67, 68). The methods used to assess treatment success suggest that tissue heating is an important feature of achieving successful vascular occlusion in this model. Hyperechoic regions, as seen at the HIFU focus in our targets, are associated with bubble formation caused by tissue water boiling (69). Development of hyperechoic regions during two or more successive exposures appeared to be a sensitive and specific marker of successful vascular occlusion, compared to the observation of structural change of the placentome, which was not a good indicator of vascular occlusion. Evidence of tissue heating was seen macroscopically where tissue pallor (suggestive of tissue denaturation) occurred in the central region of treated placentomes. Histologically, occlusion of vessel lumen with clot was observed. Together, these features suggest that achieving tissue heating within the placentome is an important process in achieving vascular occlusion.

In summary, these initial feasibility studies demonstrate the utility of ultrasound-guided HIFU to target and safely occlude placental blood vessels in vivo with a 93% success rate. This raises the prospect of non-invasive HIFU treatment of TTTS and other related conditions resulting from abnormal placental vasculature, such as twin reversed arterial perfusion (TRAP) sequence and TAPS in human pregnancy.

Materials and Methods

Study design: This animal study was designed to assess the efficacy, materno-fetal responses and safety of using high intensity focused ultrasound (HIFU) to non-invasively occlude placental vasculature, compared to sham treatment. Eleven anesthetized pregnant sheep were used in the study (5 HIFU-treated, 6 sham controls), and there was no randomization or blinding. The study was powered to detect a difference in means of ≥ 2.5 at $\alpha = 0.05$ with a power of 80%, based on published data of chronically instrumented sheep fetuses (70). The primary efficacy endpoint was achieving vascular occlusion; the primary safety endpoints were detection of uterine or fetal burns or placental hemorrhage. Maternal and fetal responses were measured using cardiovascular, acid-base, and metabolic criteria. All procedures were performed in accordance with the UK Animals (Scientific Procedures) Act 1986 and were approved by the Ethical Review Committee of the University of Cambridge.

Surgical preparation: Eleven pregnant Welsh mountain sheep with singleton fetuses at 116±2 days gestation (term ~147 days) were used. Animals were fasted for 24 hours before operation. Anesthesia was induced with alfaxalone 3mg/kg (Alfaxan, Jurox) and maintained with isoflurane (1.5-2.5% in 4:1 O_2:N_2O). Maternal oxygen saturation and end-tidal carbon dioxide ($EtCO_2$) were monitored non-invasively; $EtCO_2$ was maintained at <6%. For the procedure, the ewe was maintained in left lateral tilt. A midline abdominal incision was made and hysterotomy performed for instrumentation of the fetus. Fetal arterial catheters were introduced into the fetal carotid and femoral arteries and advanced into the ascending and descending aorta, respectively (37). A third catheter was placed in the amniotic fluid to provide a reference for "zero pressure". Time-transit flow probes were placed around the contralateral fetal carotid and femoral arteries (2 mm aperture, R-series, Transonic Systems Inc.) and on a main branch of the maternal uterine artery

at the level of the cervix (4 mm aperture, S-series, Transonic Systems Inc.). An arterial catheter was advanced into the maternal descending aorta via the femoral artery. The hysterotomy incisions were closed but the rectus sheath remained open to allow direct access for the HIFU probe to the uterine surface.

Experimental protocol: Arterial blood pressures and flows were continuously monitored using the customized Cambridge Data Acquisition System (70). Data were converted into absolute values and recorded for offline analysis (sampling rate of 500 kHz, IDEEQ, Maastricht Instruments). Mean values for sequential 1 minute epochs "minute means" were generated for cardiovascular data (Labchart 7 Pro, AD Instruments Ltd.). The experimental protocol was started within 30 minutes of completion of surgery, while the animal remained under anesthesia. It was divided into three periods. The first of these was a baseline period of 30 minutes during which the uterus was not manipulated and a static water bag containing approximately 3 L of degassed water and the diagnostic and therapeutic transducers was in contact with the uterine surface. Placental vasculature was mapped using B Mode and color Doppler ultrasound imaging (P10-4, Z. One Zonare or P10-4 Toshiba Powervision 7000). The second period consisted of 30 minutes of HIFU exposure/sham exposure of placental vasculature (a total of 6 placentomes were targeted per animal in the HIFU group with a single vessel targeted per placentome). This phase included gentle manipulation of the uterus to optimize the acoustic window. The last phase was a 30 minute recovery period, after which the animals were euthanized by terminal anesthesia. Blood samples were taken from the maternal femoral artery and the fetal femoral and carotid arteries at the start of baseline (-30 min), the start, midpoint, and end of HIFU/sham exposures, and at the end of the recovery phase (Fig. S1). We measured acid-base status, P_aO_2, and P_aCO_2 (ABL5 Blood Gas

Analyser, Radiometer); hemoglobin, hematocrit, and oxygen saturation of the blood (ABL80 Flex, Radiometer); blood glucose and lactate (YSI 2300 Stat Plus, Yellow Springs Instruments).

HIFU Protocol: HIFU was applied directly through the uterine surface, acoustically coupled using a degassed water-filled bag suspended from an arm on a positioning gantry. The Sonic Concepts H148MR transducer used (frequency 1.66 MHz, 64 mm diameter, 63 mm focal length, 19 mm central aperture for ultrasound imaging, focal diameter 1.2 mm, focal length 8.9 mm) was held in position within the water bag on an automated 3D positioning gantry (Fig. 5A). A laptop computer was used to run a graphical user interface (MATLAB R2013a, Mathworks) to control and log the automated gantry position, signal generator settings, and timing of exposures. A single line of HIFU exposures was made using the motorized gantry across the target vessel in the central region of each placentome (Fig. 5B), identified using a P 10-4 Zonare ultrasound probe centrally mounted behind the HIFU transducer. Exposure conditions were: 4-7 exposures of 5 s duration, spaced 5 s and 2 mm apart at an estimated in situ I_{SPTA} of 3900 to 5700 $W.cm^{-2}$ (table S2) based on a HIFU protocol we optimized previously and described elsewhere (61). Tissue responses such as hyperecho and structural change were recorded (3 s clips) using tissue harmonic imaging (8.0 MHz B Mode) during exposures for offline analysis. Placental vasculature was assessed and still images recorded before and immediately after HIFU exposure using color Doppler in the same 3D position, controlled by the automated gantry. Treatment success was defined as no flow detectable on color Doppler after treatment using the lowest velocity scale setting and pre-gain settings. If occlusion was incomplete, re-ablation of the same target using the same protocol was attempted once, if judged safe to do so, before exposure of a subsequent target. Mechanical ventilation pauses of up to 90 s were required during HIFU exposure series, because respiratory

movement could cause mistargeting. Ventilation was planned to be resumed before the end of a HIFU exposure series if maternal $EtCO_2$ rose to >8% or SpO_2 fell to <94%, although this did not occur.

Post-mortem and histology: Green dye was injected under ultrasound guidance into tissue adjacent to exposed placentomes for post-mortem identification. Animals were sacrificed using pentobarbitone sodium, 120 mg/kg, by rapid intravenous injection (Pentoject, Animalcare) at the completion of the HIFU protocol (within 4 hours of its start) and a post-mortem examination was conducted to identify exposed placentomes and any iatrogenic harm to the mother (examination of adjacent organs) or fetus (external examination). All treated and a smaller number of control placentomes were dissected, examined for gross pathological changes, photographed, and immersion fixed in 4% formaldehyde for 5 days before embedding in paraffin wax. Ten micrometer sections were stained with hematoxylin and eosin.

Statistical analyses: Minute means and absolute values from blood sampling are expressed as mean ± standard error of the mean (SEM). Summary measure analysis (area under the curve) was applied to the cardiovascular data for statistical analysis (71). Normality was assessed using the Shapiro Wilks test, followed by repeated measures two-way ANOVA (for time and treatment group) for parametric values and Kruskall-Wallis test for non-parametric values. In the repeated measures (RM) ANOVA, if a significant interaction was demonstrated for time or treatment, post hoc Tukey's or Sidak's test was applied. Statistical significance was accepted when $p < 0.05$.

References and notes:

1. Caloone J, Huissoud C, Vincenot J, Kocot A, Dehay C, Chapelon JY, et al. High-intensity focused ultrasound applied to the placenta using a toroidal transducer: a preliminary ex-vivo study. Ultrasound Obstet Gynecol. 2015;45(3):313-9.

2. ter Haar G, Coussios C. High intensity focused ultrasound: physical principles and devices. Int J Hyperthermia. 2007;23(2):89-104.

3. Okai T, Ichizuka K, Hasegawa J, Matsuoka R, Nakamura M, Shimodaira K, et al. First successful case of non-invasive in-utero treatment of twin reversed arterial perfusion sequence by high-intensity focused ultrasound. Ultrasound Obstet Gynecol. 2013;42(1):112-4.

4. Lewi L, Jani J, Blickstein I, Huber A, Gucciardo L, Van Mieghem T, et al. The outcome of monochorionic diamniotic twin gestations in the era of invasive fetal therapy: a prospective cohort study. Am J Obstet Gynecol. 2008;199(5):514.e1-8.

5. Saunders NJ, Snijders RJ, Nicolaides KH. Twin-twin transfusion syndrome during the 2nd trimester is associated with small intertwin hemoglobin differences. Fetal Diagn Ther. 1991;6(1-2):34-6.

6. Steinberg LH, Hurley VA, Desmedt E, Beischer NA. Acute polyhydramnios in twin pregnancies. Aust N Z J Obstet Gynaecol. 1990;30(3):196-200.

7. Denbow ML, Cox P, Taylor M, Hammal DM, Fisk NM. Placental angioarchitecture in monochorionic twin pregnancies: relationship to fetal growth, fetofetal transfusion syndrome, and pregnancy outcome. Am J Obstet Gynecol. 2000;182(2):417-26.

8. Quintero RA, Morales WJ, Allen MH, Bornick PW, Johnson PK, Kruger M. Staging of twin-twin transfusion syndrome. J Perinatol. 1999;19(8 Pt 1):550-5.

9. Senat M-V, Deprest J, Boulvain M, Paupe A, Winer N, Ville Y. Endoscopic Laser Surgery versus Serial Amnioreduction for Severe Twin-to-Twin Transfusion Syndrome. New England Journal of Medicine. 2004;351(2):136-44.

10. Ville Y, Hecher K, Ogg D, Warren R, Nicolaides K. Successful outcome after Nd : YAG laser separation of chorioangiopagus-twins under sonoendoscopic control. Ultrasound Obstet Gynecol. 1992;2(6):429-31.

11. Roberts D, Neilson JP, Kilby MD, Gates S. Interventions for the treatment of twin-twin transfusion syndrome. Cochrane Database Syst Rev. 2014;1:CD002073.

12. Rossi AC, Vanderbilt D, Chmait RH. Neurodevelopmental outcomes after laser therapy for twin-twin transfusion syndrome: a systematic review and meta-analysis. Obstet Gynecol. 2011;118(5):1145-50.

13. Robyr R, Lewi L, Salomon LJ, Yamamoto M, Bernard JP, Deprest J, et al. Prevalence and management of late fetal complications following successful selective laser coagulation of chorionic plate anastomoses in twin-to-twin transfusion syndrome. Am J Obstet Gynecol. 2006;194(3):796-803.

14. Lopriore E, Slaghekke F, Middeldorp JM, Klumper FJ, Oepkes D, Vandenbussche FP. Residual anastomoses in twin-to-twin transfusion syndrome treated with selective fetoscopic laser surgery: localization, size, and consequences. Am J Obstet Gynecol. 2009;201(1):66.e1-4.

15. Lewi L, Deprest J, Hecher K. The vascular anastomoses in monochorionic twin pregnancies and their clinical consequences. Am J Obstet Gynecol. 2013;208(1):19-30.

16. Chmait RH, Assaf SA, Benirschke K. Residual vascular communications in twin-twin transfusion syndrome treated with sequential laser surgery: frequency and clinical implications. Placenta. 2010;31(7):611-4.

17. Walsh CA, McAuliffe FM. Recurrent twin-twin transfusion syndrome after selective fetoscopic laser photocoagulation: a systematic review of the literature. Ultrasound Obstet Gynecol. 2012;40(5):506-12.

18. Zhao DP, de Villiers SF, Slaghekke F, Walther FJ, Middeldorp JM, Oepkes D, et al. Prevalence, size, number and localization of vascular anastomoses in monochorionic placentas. Placenta. 2013;34(7):589-93.

19. Hafez B, Hafez ESE. Reproduction in farm animals. Philadelphia ;London: Lippincott Williams & Wilkins; 2000. 509 p.

20. Nikkels PG, Hack KE, van Gemert MJ. Pathology of twin placentas with special attention to monochorionic twin placentas. J Clin Pathol. 2008;61(12):1247-53.

21. Wooding FBP, Burton G. Comparative placentation : structures, functions and evolution. Berlin: Springer; 2008.

22. Barry JS, Anthony RV. The pregnant sheep as a model for human pregnancy. Theriogenology. 2008;69(1):55-67.

23. De Lia JE, Cruikshank DP, Keye WR, Jr. Fetoscopic neodymium:YAG laser occlusion of placental vessels in severe twin-twin. Obstet Gynecol. 1990;75(6):1046-53.

24. Rueda-Clausen CF, Morton JS, Davidge ST. The early origins of cardiovascular health and disease: who, when, and how. Semin Reprod Med. 2011;29(3):197-210.

25. McClaine RJ, Uemura K, de la Fuente SG, Manson RJ, Booth JV, White WD, et al. General anesthesia improves fetal cerebral oxygenation without evidence of subsequent neuronal injury. J Cereb Blood Flow Metab. 2005;25(8):1060-9.

26. McClaine RJ, Uemura K, McClaine DJ, Shimazutsu K, de la Fuente SG, Manson RJ, et al. A description of the preterm fetal sheep systemic and central responses to maternal general anesthesia. Anesth Analg. 2007;104(2):397-406.

27. Biehl DR, Yarnell R, Wade JG, Sitar D. The uptake of isoflurane by the foetal lamb in utero: effect on regional blood flow. Can Anaesth Soc J. 1983;30(6):581-6.

28. Gaynor JS, Wertz EM, Alvis M, Turner AS. A comparison of the haemodynamic effects of propofol and isoflurane in pregnant ewes. J Vet Pharmacol Ther. 1998;21(1):69-73.

29. Baker BW, Hughes SC, Shnider SM, Field DR, Rosen MA. Maternal anesthesia and the stressed fetus: effects of isoflurane on the asphyxiated fetal lamb. Anesthesiology. 1990;72(1):65-70.

30. Bachman CR, Biehl DR, Sitar D, Cumming M, Pucci W. Isoflurane potency and cardiovascular effects during short exposures in the foetal lamb. Can Anaesth Soc J. 1986;33(1):41-7.

31. Palahniuk RJ, Shnider SM. Maternal and fetal cardiovascular and acid-base changes during halothane and isoflurane anesthesia in the pregnant ewe. Anesthesiology. 1974;41(5):462-72.

32. Quick AJ. Hemostasis in surgical procedures. Surg Gynecol Obstet. 1969;128(3):523-32.

33. Giussani DA. The fetal brain sparing response to hypoxia: physiological mechanisms. J Physiol. 2016;594(5):1215-30.

34. Stein P, White SE, Homan J, Hanson MA, Bocking AD. Altered fetal cardiovascular responses to prolonged hypoxia after sinoaortic denervation. Am J Physiol. 1999;276(2 Pt 2):R340-6.

35. Challis JR, Fraher L, Oosterhuis J, White SE, Bocking AD. Fetal and maternal endocrine responses to prolonged reductions in uterine blood flow in pregnant sheep. Am J Obstet Gynecol. 1989;160(4):926-32.

36. Bocking AD, Gagnon R, White SE, Homan J, Milne KM, Richardson BS. Circulatory responses to prolonged hypoxemia in fetal sheep. Am J Obstet Gynecol. 1988;159(6):1418-24.

37. Giussani DA, Spencer JA, Moore PJ, Bennet L, Hanson MA. Afferent and efferent components of the cardiovascular reflex responses to acute hypoxia in term fetal sheep. J Physiol. 1993;461:431-49.

38. Hill EPPGGLLD. A mathematical model of carbon dioxide transfer in the placenta and its interaction with oxygen. American Journal of Physiology -- Legacy Content. 1973;224(2):283-99.

39. Barnard JM, Chaffin D, Droste S, Tierney A, Phernetton T. Fetal response to carbon dioxide pneumoperitoneum in the pregnant ewe. Obstet Gynecol. 1995;85(5 Pt 1):669-74.

40. Cruz AM, Southerland LC, Duke T, Townsend HG, Ferguson JG, Crone LA. Intraabdominal carbon dioxide insufflation in the pregnant ewe. Uterine blood flow, intraamniotic pressure, and cardiopulmonary effects. Anesthesiology. 1996;85(6):1395-402.

41. Bhavani-Shankar K, Steinbrook RA, Brooks DC, Datta S. Arterial to end-tidal carbon dioxide pressure difference during laparoscopic surgery in pregnancy. Anesthesiology. 2000;93(2):370-3.

42. Ganong WF. Review of medical physiology. Stamford, Conn.: McGraw Hill; 2001.

43. Low JA, Pancham SR, Worthington D, Boston RW. The acid-base and biochemical characteristics of intrapartum fetal asphyxia. Am J Obstet Gynecol. 1975;121(4):446-51.

44. Martin RW, Vaezy S, Kaczkowski P, Keilman G, Carter S, Caps M, et al. Hemostasis of punctured vessels using Doppler-guided high-intensity ultrasound. Ultrasound Med Biol. 1999;25(6):985-90.

45. Jiao J, Wu F, Zou J, Li F, Liu F, Zhao X, et al. [Effect of ablations by pulsed versus continuous high-intensity focused ultrasound on isolated perfused porcine liver]. Nan Fang Yi Ke Da Xue Xue Bao. 2013;33(2):230-4.

46. Hynynen K, Colucci V, Chung A, Jolesz F. Noninvasive arterial occlusion using MRI-guided focused ultrasound. Ultrasound Med Biol. 1996;22(8):1071-7.

47. Kim Y, Gelehrter SK, Fifer CG, Lu JC, Owens GE, Berman DR, et al. Non-invasive pulsed cavitational ultrasound for fetal tissue ablation: feasibility study in a fetal sheep model. Ultrasound Obstet Gynecol. 2011;37(4):450-7.

48. Rivens IH, Rowland IJ, Denbow M, Fisk NM, ter Haar GR, Leach MO. Vascular occlusion using focused ultrasound surgery for use in fetal medicine. Eur J Ultrasound. 1999;9(1):89-97.

49. Delon-Martin C, Vogt C, Chignier E, Guers C, Chapelon JY, Cathignol D. Venous thrombosis generation by means of high-intensity focused ultrasound. Ultrasound Med Biol. 1995;21(1):113-9.

50. Acharya G, Erkinaro T, Mäkikallio K, Lappalainen T, Rasanen J. Relationships among Doppler-derived umbilical artery absolute velocities, cardiac function, and placental volume blood flow and resistance in fetal sheep. Am J Physiol Heart Circ Physiol. 2004;286(4):H1266-72.

51. Morel O, Pachy F, Chavatte-Palmer P, Bonneau M, Gayat E, Laigre P, et al. Correlation between uteroplacental three-dimensional power Doppler indices and true uterine blood flow: evaluation in a pregnant sheep model. Ultrasound Obstet Gynecol. 2010;36(5):635-40.

52. Taylor MJ, Farquharson D, Cox PM, Fisk NM. Identification of arterio-venous anastomoses in vivo in monochorionic twin pregnancies: preliminary report. Ultrasound Obstet Gynecol. 2000;16(3):218-22.

53. Machin GA, Feldstein VA, van Gemert MJ, Keith LG, Hecher K. Doppler sonographic demonstration of arterio-venous anastomosis in monochorionic twin gestation. Ultrasound Obstet Gynecol. 2000;16(3):214-7.

54. Wee LY, Sullivan M, Humphries K, Fisk NM. Longitudinal blood flow in shared (arteriovenous anastomoses) and non-shared cotyledons in monochorionic placentae. Placenta. 2007;28(5-6):516-22.

55. Ruano R, Rodo C, Peiro JL, Shamshirsaz AA, Haeri S, Nomura ML, et al. Fetoscopic laser ablation of placental anastomoses in twin-twin transfusion syndrome using 'Solomon technique'. Ultrasound Obstet Gynecol. 2013;42(4):434-9.

56. Shaw CJ, ter Haar GR, Rivens IH, Giussani DA, Lees CC. Pathophysiological mechanisms of high-intensity focused ultrasound-mediated vascular occlusion and relevance to non-invasive fetal surgery. J R Soc Interface. 2014;11(95):20140029.

57. Denbow ML, Rivens IH, Rowland IJ, Leach MO, Fisk NM, ter Haar GR. Preclinical development of noninvasive vascular occlusion with focused ultrasonic surgery for fetal therapy. Am J Obstet Gynecol. 2000;182(2):387-92.

58. Hynynen K, Chung AH, Colucci V, Jolesz FA. Potential adverse effects of high-intensity focused ultrasound exposure on blood vessels in vivo. Ultrasound Med Biol. 1996;22(2):193-201.

59. Mahoney K, Martin H, Hynynen K, editors. Focused ultrasound effects on blood vessels in vivo-limits for vascular interventions. Ultrasonics Symposium, 2000 IEEE; 2000 Oct 2000.

60. Vaezy S, Martin R, Kaczkowski P, Keilman G, Goldman B, Yaziji H, et al. Use of high-intensity focused ultrasound to control bleeding. J Vasc Surg. 1999;29(3):533-42.

61. Shaw C, Civale J, Giussani D, Rivens I, Ter Haar G, Lees C. OC18.07: Ultrasound-guided high intensity focused ultrasound (HIFU) ablation of placental vasculature. Ultrasound in Obstetrics & Gynecology. 2015;46:39-40.

62. Effects of antenatal dexamethasone administration in the infant: long-term follow-up. J Pediatr. 1984;104(2):259-67.

63. ter Haar GR, Robertson D. Tissue destruction with focused ultrasound in vivo. Eur Urol. 1993;23 Suppl 1:8-11.

64. Chen SS, Wright NT, Humphrey JD. Heat-Induced Changes in the Mechanics of a Collagenous Tissue: Isothermal Free Shrinkage. 1997;119(4):372-8.

65. Tokarczyk A, Rivens I, van Bavel E, Symonds-Tayler R, ter Haar G. An experimental system for the study of ultrasound exposure of isolated blood. Phys Med Biol. 2013;58(7):2281-304.

66. White RA, Kopchok G, Peng SK, Fujitani R, White G, Klein S, et al. Laser vascular welding--how does it work? Ann Vasc Surg. 1987;1(4):461-4.

67. Hwang JH, Vaezy S, Martin RW, Cho MY, Noble ML, Crum LA, et al. High-intensity focused US: a potential new treatment for GI bleeding. Gastrointest Endosc. 2003;58(1):111-5.

68. Ishikawa T, Okai T, Sasaki K, Umemura S, Fujiwara R, Kushima M, et al. Functional and histological changes in rat femoral arteries by HIFU exposure. Ultrasound Med Biol. 2003;29(10):1471-7.

69. McLaughlan J, Rivens I, Leighton T, Ter Haar G. A study of bubble activity generated in ex vivo tissue by high intensity focused ultrasound. Ultrasound Med Biol. 2010;36(8):1327-44.

70. Allison BJ, Brain KL, Niu Y, Kane AD, Herrera EA, Thakor AS, et al. Fetal in vivo continuous cardiovascular function during chronic hypoxia. J Physiol. 2016;594(5):1247-64.

71. Matthews JN, Altman DG, Campbell MJ, Royston P. Analysis of serial measurements in medical research. Bmj. 1990;300(6719):230-5.

Funding: Supported by Action Medical Research grant no. GN2052, the Isaac Newton Trust, Genesis Research Trust. G.tH. and I.R. are supported by Focused Ultrasound Foundation Centre of Excellence. Professor D. A. Giussani is supported by the British Heart Foundation. Dr C.C.Lees is supported by the National Institute for Health Research (NIHR) Biomedical Research Centre based at Imperial College Healthcare NHS Trust and Imperial College London. The views expressed are those of the author(s) and not necessarily those of the NHS, the NIHR or the Department of Health.

Author Contributions: C.J.S, I.R, D.A.G. contributed to paper, designed and performed experiments. C.C.L. and G.tH. contributed to paper and designed experiments. K.J.B., Y.N. and J.C. performed all experiments. J.C. created software for automated gantry control and image analysis.

Competing interests: The authors declare that they have no competing interests.

Tables:

Variable	Treatment Group	Baseline (-30 min)	(0 min)	Exposure Series (15 min)	(30 min)	Recovery (60 min)	p value (* time)	p value († treatment)
pH	HIFU	7.51 ± 0.02	7.50 ± 0.03	7.47 ± 0.03	7.49 ± 0.01 †	7.51 ± 0.02 †	0.27	0.007
	Sham	7.44 ± 0.01	7.43 ± 0.01	7.42 ± 0.01	7.40 ± 0.02	7.40 ± 0.02		
Arterial Base Excess (mmol.L-1)	HIFU	8.2 ± 0.9	7.6 ± 0.7	7.4 ± 0.8	7.6 ± 0.8	7.2 ± 0.6	0.86	0.16
	Sham	4.8 ± 1.5	5.7 ± 1.1	5.5 ± 1.0	5.7 ± 1.1	5.3 ± 1.3		
pCO2 (mmHg)	HIFU	40.0 ± 1.6	42.0 ± 3.4	43.8 ± 3.7	41.8 ± 1.0 †	38.6 ± 2.9 †	0.17	0.048
	Sham	48.7 ± 2.2	49.0 ± 4.0	54.3 ± 2.0	54.3 ± 1.3	52.7 ± 1.8		
Lactate (mmol.L-1)	HIFU	1.2 ± 0.2	1.1 ± 0.2	1.1 ± 0.1	1.0 ± 0.1	1.1 ± 0.2	0.16	0.09
	Sham	0.7 ± 0.1	0.6 ± 0.1	0.6 ± 0.1	0.6 ± 0.1	0.6 ± 0.1		
Bicarbonate (mEq.L-1)	HIFU	32.0 ± 1.0	31.8 ± 1.1	31.8 ± 0.8	31.7 ± 0.8	31.0 ± 1.0	0.32	0.84
	Sham	30.8 ± 1.4	31.8 ± 1.4	31.8 ± 1.3	31.8 ± 1.3	31.8 ± 1.3		
pO2 (mmHg)	HIFU	216.0 ± 47.5	200.4 ± 67.3	190.4 ± 74.2	186.2 ± 72.4	218.2 ± 64.2	0.60	0.71
	Sham	198.8 ± 25.4	169.8 ± 22.8	163.8 ± 23.4	183.3 ± 32.3	180.0 ± 26.2		
Oxyhemoglobin Saturation (%)	HIFU	102.3 ± 1.2	100.1 ± 2.2	97.6 ± 3.0	101.1 ± 1.6	101.9 ± 1.6	0.77	0.96
	Sham	95.1 ± 7.8	102.3 ± 1.3	102.0 ± 1.5	101.3 ± 1.9	102.4 ± 1.1		
	HIFU	8.0 ± 0.4	7.8 ± 0.4	8.0 ± 0.5	8.2 ± 0.4	8.6 ± 0.3	0.048	0.08

Hemoglobin (g.dL-1)	Sham	8.9 ± 0.6	9.0 ± 0.5	9.1 ± 0.5	9.6 ± 0.3	9.7 ± 0.4 *		
Hematocrit	HIFU	0.24 ± 0.01	0.24 ± 0.02	0.25 ± 0.02	0.25 ± 0.01	0.26 ± 0.01	0.0003	0.73
	Sham	0.24 ± 0.01	0.24 ± 0.01	0.25 ± 0.01	0.28 ± 0.01 *	0.28 ± 0.01*		

Table 1: Maternal arterial acid base and metabolic status

Values represent mean ± SEM of maternal femoral arterial blood sampled at the start of the baseline period (-30 min), the start, middle, and end of the HIFU (n=5) or sham (n=6) exposure series (0, 15, 30 min), and the end of the recovery period (60 min). Significant differences are indicated as *$p<0.05$ for the effect of time vs. baseline; $^{\dagger}p<0.05$ for the effect of treatment group, repeated measures two-way ANOVA with post hoc Tukey and Sidak tests.

Variable	Treatment Group	Baseline (-30 min)	Exposure Series (0 min)	(15 min)	(30 min)	Recovery (60 min)	p value (* time)	p value († treatment)
pH	HIFU	7.27 ± 0.01	7.28 ± 0.01 †	7.26 ± 0.02 †	7.23 ± 0.01 *	7.18 ± 0.02*	< 0.0001	0.02
	Sham	7.21 ± 0.03	7.21 ± 0.02	7.18 ± 0.02	7.17 ± 0.02 *	7.15 ± 0.03*		
Arterial Base Excess (mmol.L-1)	HIFU	-0.4 ± 0.9	-0.2 ± 0.6	-0.6 ± 0.7	-1.8 ± 0.4	-4.4 ± 0.7 *	0.003	0.73
	Sham	-1.2 ± 1.6	-0.8 ± 0.8	-2.2 ± 0.7	-2.3 ± 0.8	-2.5 ± 1.2 *		
pCO2 (mmHg)	HIFU	62.4 ± 3.7	61.8 ± 5.5	70.4 ± 11.4	69.4 ± 7.4	77.6 ± 6.9 *	0.003	0.30
	Sham	73.0 ± 4.3	76.5 ± 2.8	75.8 ± 3.5	75.3 ± 3.9	80.5 ± 5.5 *		
Lactate (mmol.L-1)	HIFU	2.3 ± 0.4	2.2 ± 0.3	2.2 ± 0.3	2.8 ± 0.4	3.0 ± 0.4 *	0.0003	0.12
	Sham	1.7 ± 0.2	1.7 ± 0.2	1.8 ± 0.2	1.8 ± 0.2	2.3 ± 0.3 *		
Bicarbonate (mEq.L-1)	HIFU	25.6 ± 1.3	26.4 ± 0.8	25.2 ± 0.8	25.0 ± 0.6	24.6 ± 0.2	0.22	0.91
	Sham	27.8 ± 1.7	28.7 ± 0.9	27.5 ± 1.3	27.7 ± 1.2	27.8 ± 0.8		
pO2 (mmHg)	HIFU	25.2 ± 1.1	25.0 ± 2.8	23.8 ± 3.3	23.0 ± 3.2	18.4 ± 0.9 *	< 0.0001	0.21
	Sham	27.2 ± 1.2	28.3 ± 1.2	27.7 ± 1.2	26.3 ± 1.9	22.3 ± 1.9 *		
Oxyhemoglobin saturation (%)	HIFU	72.8 ± 1.1	72.3 ± 2.9	69.3 ± 8.3	66.3 ± 7.4	46.8 ± 2.8 *	< 0.0001	0.62
	Sham	70.4 ± 7.5	64.8 ± 2.9	64.3 ± 3.9	63.1 ± 4.7	51.2 ± 9.5 *		
Hemoglobin (g.dL-1)	HIFU	10.0 ± 0.2	10.2 ± 0.2	10.7 ± 0.3	11.0 ± 0.5	11.1 ± 0.2 *	0.0026	0.06
	Sham	9.3 ± 0.2	10.5 ± 0.3	9.8 ± 0.2	10.0 ± 0.2	10.7 ± 0.4 *		
Hematocrit	HIFU	0.32 ± 0.01	0.33 ± 0.01	0.34 ± 0.02	0.35 ± 0.01 *	0.35 ± 0.01*	0.03	0.55
	Sham	0.27 ± 0.02	0.34 ± 0.02	0.32 ± 0.02	0.34 ± 0.02 *	0.33 ± 0.03*		

Table 2: Fetal arterial acid base and metabolic status

Values represent mean ± SEM of fetal carotid arterial blood sampled at the start of the baseline period (-30 min), the start, middle, and end of the HIFU (n=5) or sham (n=6) exposure series (0, 15, 30 min), and the end of the recovery period (60 min). Significant differences are indicated as *$p<0.05$ for the effect of time vs. baseline, $^{\dagger}p<0.05$ for the effect of treatment group, repeated measures two-way ANOVA with post hoc Tukey and Sidak tests.

Variable	Treatment Group	Baseline (-30 min)	Exposure Series (0 min)	(15 min)	(30 min)	Recovery (60 min)	p value (* time)	p value († treatment)
Carotid Arterial Oxygen Delivery (mmol.min-1)	HIFU	383 ± 30	374 ± 39	373 ± 41	352 ± 28	283 ± 19	0.21	0.63
	Sham	359 ± 82	361 ± 40	312 ± 37	334 ± 50	281 ± 33		
Femoral Arterial Oxygen Delivery (mmol.min-1)	HIFU	116 ± 9	106 ± 13	73 ± 15 *	67 ± 12 *	55 ± 8 *	< 0.0001	0.28
	Sham	114 ± 14	116 ± 13	82 ± 10 *	99 ± 10 *	91 ± 18 *		
Carotid : Femoral Oxygen Delivery Ratio	HIFU	3.1 ± 0.4	3.2 ± 0.2	4.8 ± 0.6	5.2 ± 1.1 *	4.6 ± 0.3	0.04	0.33
	Sham	3.7 ± 1.0	3.3 ± 0.5	4.0 ± 0.7	3.3 ± 0.7	3.0 ± 0.4		
Carotid Arterial Glucose Delivery (µmol.min-1)	HIFU	61 ± 14	57 ± 16	64 ± 15	77 ± 19	72 ± 13	0.59	0.74
	Sham	78 ± 14	75 ± 12	72 ± 14	67 ± 16	74 ± 19		
Femoral Arterial Glucose Delivery (µmol.min-1)	HIFU	21 ± 3	19 ± 3	15 ± 2 *	16 ± 3 *	19 ± 4	0.003	0.17
	Sham	30 ± 6	26 ± 3	19 ± 3 *	24 ± 4 *	24 ± 3		
Carotid : Femoral Glucose Delivery Ratio	HIFU	3.0 ± 0.4	2.9 ± 0.3	4.2 ± 0.8 *	4.7 ± 0.7 *	4.0 ± 0.2	0.0004	0.26
	Sham	2.6 ± 0.4	2.7 ± 0.3	3.9 ± 0.7 *	2.9 ± 0.5 *	3.0 ± 0.5		

Table 3: Fetal substrate delivery

Values represent mean ± SEM of fetal carotid and femoral arterial blood sampled at the start of the baseline period (-30 min), the start, middle, and end of the HIFU (n=5) or sham (n=6) exposure series (0, 15, 30 min), and the end of the recovery period

(60 min). Significant differences are indicated as *$p<0.05$ for the effect of time vs. baseline, RM two-way ANOVA with post hoc Tukey test.

Figures:

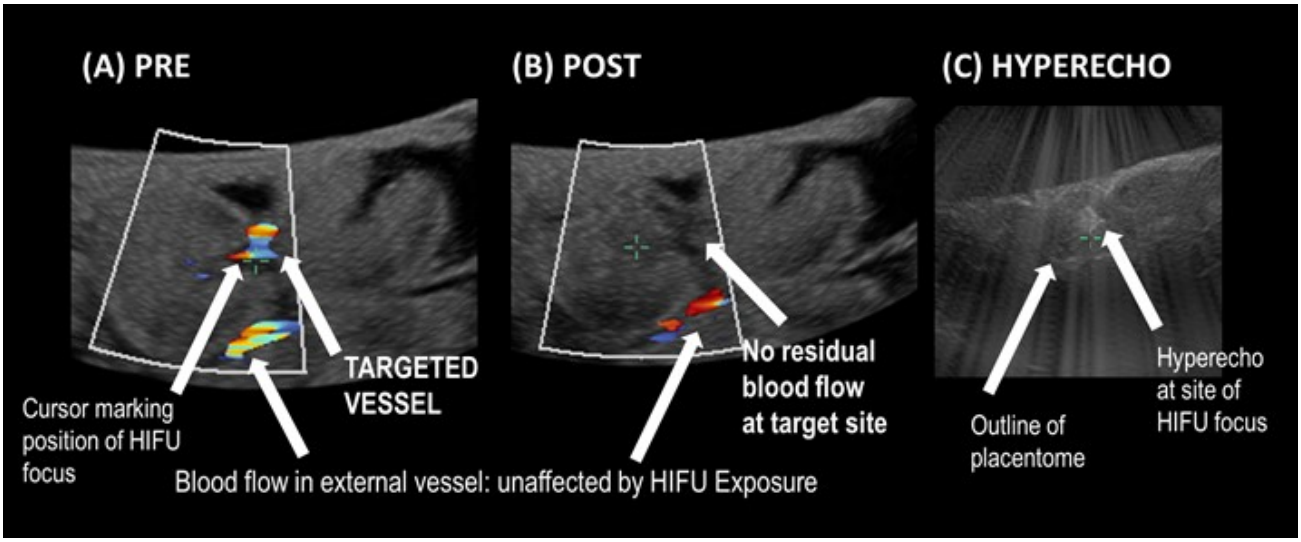

Fig. 1. **Color Doppler and B-Mode ultrasound imaging of placental vascular ablation**

(A) Pre-treatment color Doppler imaging of a placentome. The intended vascular target is indicated by an arrow. **(B)** Post-treatment color Doppler imaging of the same placentome demonstrating "no flow" within the targeted vessel; **(C)** B-mode harmonic ultrasound imaging of hyperechoic region within the HIFU focal zone.

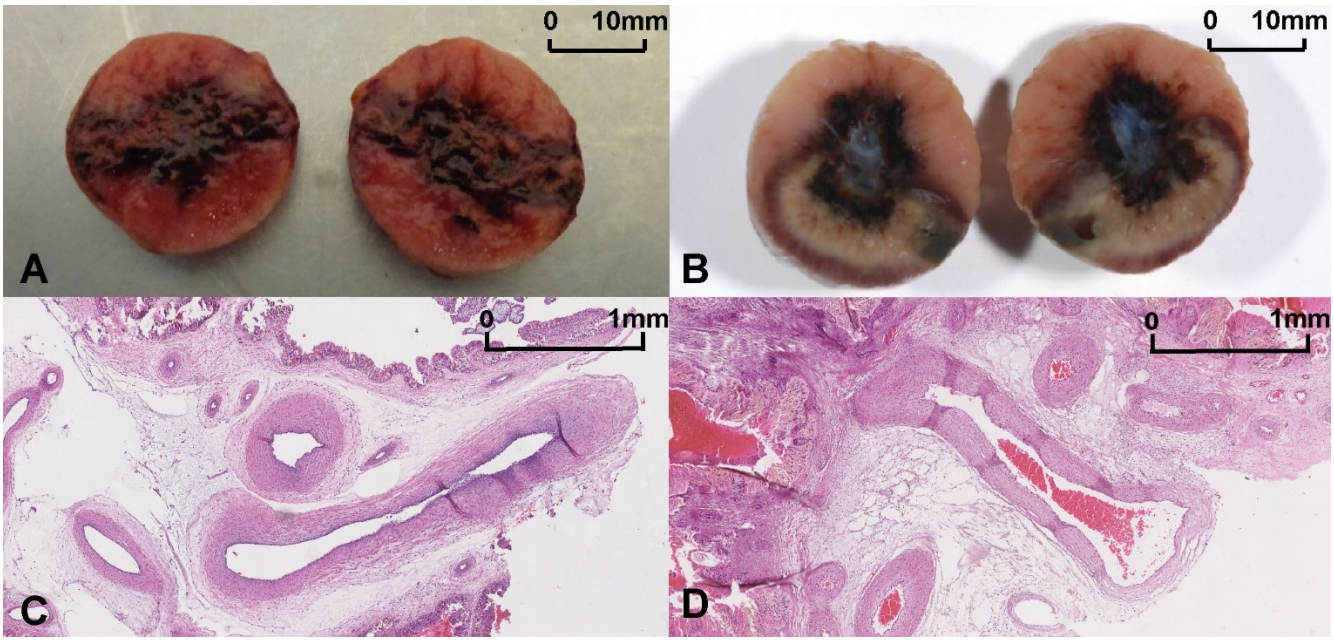

Fig. 2. Macroscopic and microscopic results of HIFU exposures

(A) Tissue darkening and **(B)** tissue pallor involving the central area of a bisected placentome. **(C)** H&E section (scale bar 1 mm) of fetal vessels in control placentome. **(D)** H&E section (scale bar 1 mm) of fetal vessels in HIFU-exposed placentome, showing clot-filled vessel lumen.

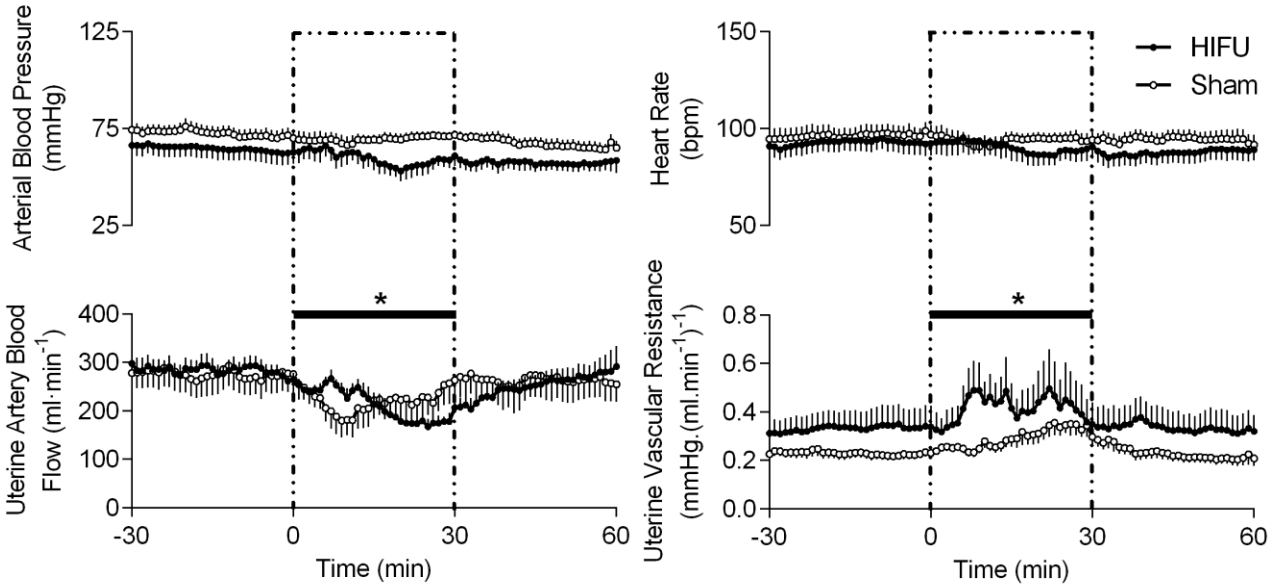

Figure 3: Maternal cardiovascular responses to HIFU or sham placental vascular ablation

The graphs show mean values for each sequential minute ± SEM of percentage change from baseline during the baseline (-30-0 min), HIFU (n=5) or sham (n=6) ablation of placental vasculature (dashed box, 0-30 min), and recovery (30-60 min) periods. Black bar indicates the timing of significant change from baseline. Significant differences: * $p<0.05$ time vs. baseline; repeated measures two way ANOVA with post hoc Tukey test.

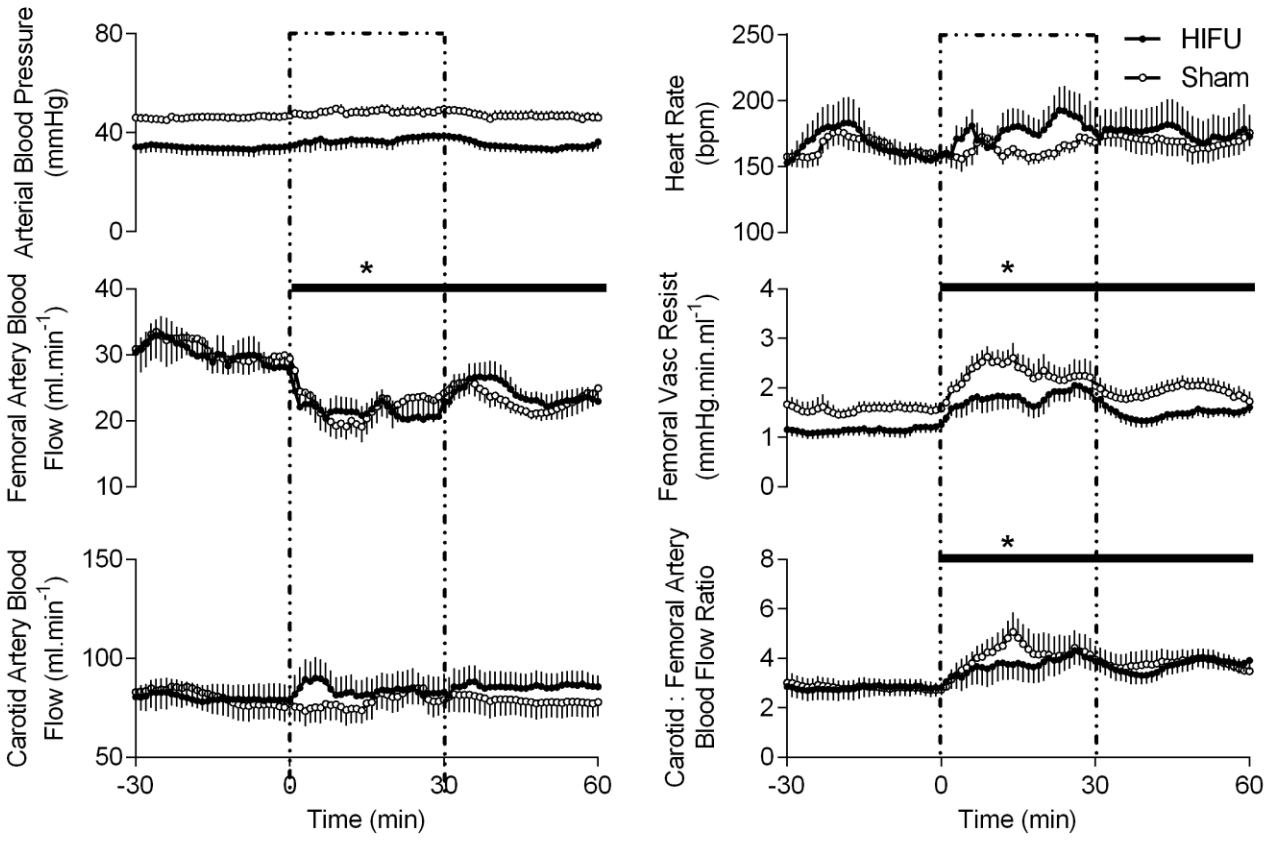

Figure 4: Fetal cardiovascular responses to HIFU or sham placental vascular ablation

The graphs show mean values for each sequential minute ± SEM of percentage change from baseline during the baseline (-30-0 min), HIFU (n=5) or sham (n=6) ablation of placental vasculature (dashed box, 0-30 min), and recovery (30-60 min) periods while under general anaesthesia. Black bar indicates the timing of significant change from baseline. Significant differences: * $p<0.05$ time vs. baseline; repeated measures two way ANOVA with post hoc Tukey test.

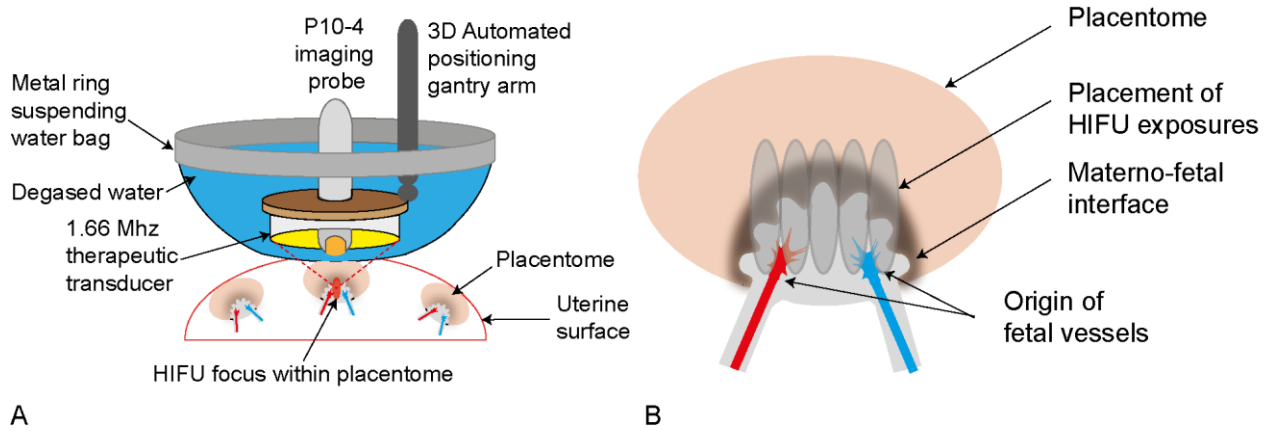

Figure 5: Diagram of side view of equipment setup and HIFU exposure placement

(A) Setup of the ring-shaped HIFU transducer and central diagnostic ultrasound probe within a bag of degassed water. **(B)** Placement of HIFU lesions in a linear track across the origin of the fetal vessels.

Supplementary Materials:

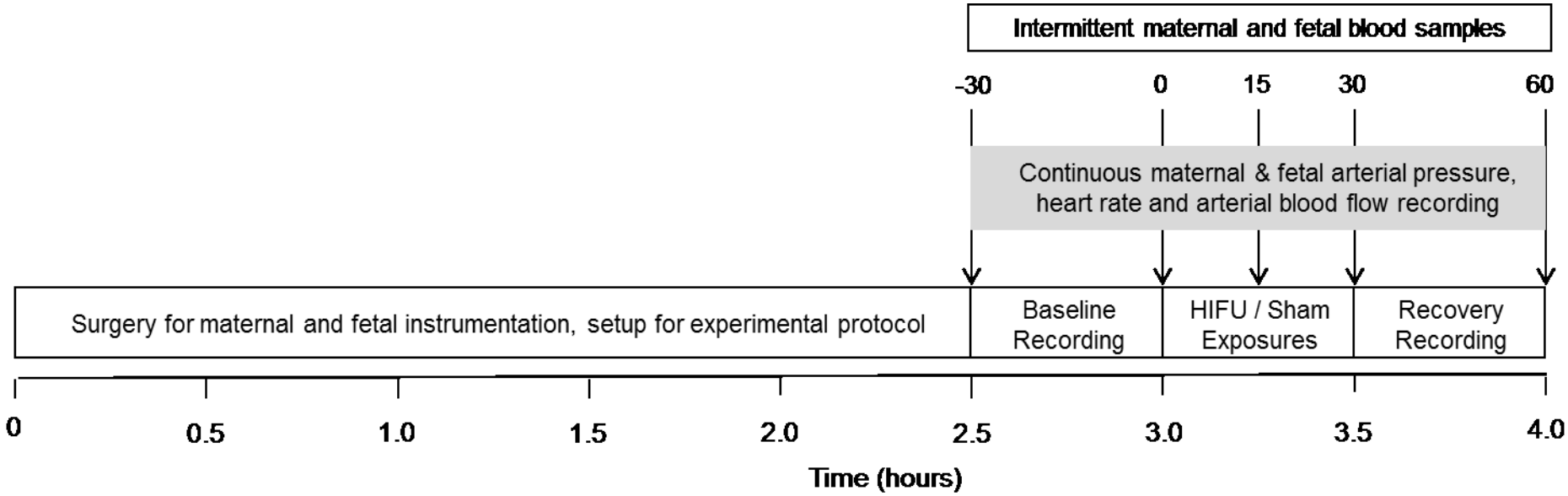

Figure S1: Surgical and experimental timeline

Schema of experimental timeline showing total length of general anaesthesia divided into time for surgical and experimental procedures, including the baseline, HIFU/sham exposures, and recovery periods.

Placentome number	Harmonic US		Doppler US		Photography		Histology					Successful treatment outcome? (of 3 criteria)	Complications
	Hyperecho (>2 successive B Mode)	Structural change (B Mode)	"No flow" color Doppler	Retreatment needed	Tissue paling (visual)	Tissue darkening (visual)	Clot in vessel	Shrunken / collapsed vessels	Cellular debris	Extravas-ation	Cross-sectional area damaged (%)		
1	Yes	Yes	Yes	No	Yes	Yes	Yes	Yes	Yes	Yes	59	Yes	None
2	Yes	Yes	Yes	No	Yes	Yes	Yes	No	Yes	Yes	23	Yes	None
3	Yes	Yes	Yes	No	Yes	Yes	Yes	No	No	Yes	27	Yes	None
4	Yes	Yes	Yes	No	Yes	Yes	Yes	No	Yes	Yes	9	Yes	None
5	Yes	No	Yes	No	Yes	Yes	Yes	Yes	Yes	Yes	30	Yes	None
6	Yes	Yes	Yes	No	No	Yes	Tissue too friable to obtain sections					2/3 criteria	None
7	Yes	No	Yes	No	Yes	No	No clear view		Yes	Yes	19	2/3 criteria	None
8	Yes	Yes	Yes	No	No	Yes	No clear view		No	Yes	34	2/3 criteria	None
9	Yes	No	Yes	No	Yes	Yes	Yes	No	Yes	Yes	24	Yes	None
10	No	No	No	Yes	Yes	Yes	Yes	No	Yes	Yes	41	No	Tissue damage involved edge of placentome; no damage to uterus, adjacent placentomes, mother, or fetus
10 (retreat)	Yes	No	Yes	No								Yes	
11	No	No	No	Not attempted	Yes	Yes	No	No	Yes	Yes	16	No	None
12	Yes	No	Yes	No	Yes	Yes	Yes	No	Yes	Yes	22	Yes	None
13	Yes	No	Yes	No	Yes	Yes	Yes	No	Yes	Yes	41	Yes	None
14	Yes	No	Yes	No	Yes	Yes	Yes	No	Yes	Yes	48	Yes	None
15	Yes	No	Yes	No	Yes	Yes	No	Yes	Yes	Yes	13	Yes	None
16	Yes	No	Yes	No	Yes	Yes	Yes	No	Yes	Yes	15	Yes	None
17	Yes	Yes	Yes	No	Yes	Yes	Yes	No	Yes	Yes	53	Yes	None
18	Yes	Yes	Yes	No	Yes	Yes	Yes	Yes	Yes	Yes	41	Yes	None
19	Yes	No	Yes	No	Yes	Yes	Yes	Yes	Yes	Yes	63	Yes	None
20	No	Yes	No	Yes	Yes	Yes	No	No	Yes	Yes	44	No	Vessel hemorrhage after 1st exposure series, not resolved by retreatment
20 (retreat)	Yes	Yes	No	Not attempted									
21	Yes	Yes	Yes	No	Yes	Yes	Yes	Yes	Yes	Yes	5	Yes	None
22	Yes	Yes	Yes	No	Yes	No	Yes	Yes	Yes	Yes	33	Yes	None
23	Yes	No	Yes	No	Yes	Yes	Yes	Yes	Yes	Yes	46	Yes	None
24	Yes	Yes	Yes	No	Yes	No	Yes	Yes	Yes	Yes	31	Yes	None
25	Yes	No	Yes	No	Yes	Yes	Yes	No	Yes	Yes	46	Yes	None

26	Yes	No	Yes	No	No	Yes	Yes	Yes	Yes	Yes	39	Yes	None
27	Yes	Yes	Yes	No	Yes	Yes	Yes	Yes	Yes	Yes	43	Yes	None
28	Yes	No	Yes	No	No	Yes	Yes	Yes	Yes	Yes	20	Yes	None
29	Yes	Yes	Yes	No	No	Yes	Yes	Yes	Yes	Yes	30	Yes	None
30	Yes	Yes	Yes	No	No	Yes	Tissue too friable to obtain sections					2/3 criteria	None

Table S1: Summary of treatment outcomes.
Outcomes and complications determined by tissue responses seen on harmonic and Doppler ultrasound imaging, visual examination, and photography at post-mortem and histological examination of tissues.

Placentome number	Exposures								
	Power (dBm)	In Situ I_{SPTA} ($W.cm^{-2}$)	Duration (s)	Interval (s)	Linear movement gantry (mm)	Depth of target (mm)	Number of exposures	Number of breath holds	Time to complete treatment (s)
1	-5	3959	5	5	12	27	7	1	136
2	-5	5537	5	5	12	10	7	1	119
3	-5	5359	5	5	18	11	10	1	135
4	-5	5521	5	5	8	10	5	1	165
5	-5	5117	5	5	6	14	4	1	105
6	-5	5560	5	5	8	9	5	1	93
7	-5	5689	5	5	8	8	5	1	81
8	-5	5547	5	5	10	10	6	1	92
9	-5	4884	5	5	8	16	5	1	106
10	-5	5005	5	5	8	16	5	1	137
10 (retreat)	-5	4832	5	5	8	16	5	1	182
11	-5	4506	5	5	10	20	6	1	99
12	-5	4579	5	5	12	19	7	1	114
13	-5	5184	5	5	10	13	6	1	142
14	-5	5053	5	5	12	14	7	1	111
15	-5	5107	5	5	8	14	5	1	92
16	-5	5059	5	5	10	14	6	1	88
17	-5	5070	5	5	12	14	7	1	146
18	-5	5124	5	5	10	14	6	1	95
19	-5	5241	5	5	8	13	5	1	89
20	-5	5337	5	5	2	12	6	1	134
20 (retreat)	-5	5442	5	5	10	12	6	1	359
21	-5	5385	5	5	10	11	6	1	107
22	-5	5168	5	5	10	13	6	1	125
23	-5	5137	5	5	8	14	5	1	70
24	-5	5015	5	5	10	15	6	1	87
25	-5	5541	5	5	8	10	5	1	84
26	-5	5561	5	5	8	9	5	1	89
27	-5	5605	5	5	10	9	6	1	97
28	-5	5583	5	5	8	9	5	1	86
29	-5	4963	5	5	8	15	5	1	128
30	-5	4546	5	5	12	20	7	1	100

Table S2: Summary of exposure conditions.
Exposure conditions used to attempt placental vascular occlusion in the 30 placental targets described in this paper.